HHS Public Access

Author manuscript

Neuropsychologia. Author manuscript; available in PMC 2021 September 17.

Published in final edited form as:

Neuropsychologia. 2021 September 17; 160: 107979. doi:10.1016/j.neuropsychologia.2021.107979.

Widespread Theta Coherence during Spatial Cognitive Control

John C. Myers[1,4,*], **Lisa K. Chinn**[1,2], **Sandeepa Sur**[5], **Edward J. Golob**[1,3]

[1]Department of Psychology, Tulane University, New Orleans, LA, 70118

[2]Texas Institute for Measurement, Evaluation, and Statistics, University of Houston, Houston, TX, 77004

[3]Department of Psychology, University of Texas, San Antonio, TX, 78249

[4]Department of Neurosurgery, Baylor College of Medicine, Houston, TX, 77030

[5]Department of Radiology, Johns Hopkins University, Baltimore, MD, 21205

Abstract

Cognitive control allows humans to process relevant sensory information while minimizing distractions from irrelevant stimuli. The neural basis of cognitive control is known to involve frontal regions of the brain such as the medial prefrontal cortex (mPFC) and anterior cingulate cortex (ACC), but the temporal dynamics of larger scale networks is unclear. Here we used EEG with source localization to identify how the neural oscillations localized to the mPFC and ACC coordinate with parietal, sensory, and motor areas during spatial cognitive control. Theta coherence (3-8 Hz) between the mPFC and ACC increased with task difficulty and predicted individual differences in reaction time. Individual differences in accuracy were predicted by earlier activation of ACC-motor coherence, highlighting the relationship between processing speed and task performance. Our results provide evidence that successful cognitive control requires dynamic coordination between a widespread network of brain regions. Long range theta coherence may be a key mechanism for efficient cognitive control across the neocortex.

Keywords

cognitive control; neuronal coherence; theta oscillations; spatial attention

The world is a noisy place, but luckily our brains can selectively process task-relevant information while filtering out things that are less relevant. This ability, known as cognitive control, adjusts dynamically across time to meet dynamically-changing task demands and goals (Chinn, Pauker, & Golob, 2018; Risko, Blais, Stolz, & Besner, 2008; Stürmer, Leuthold, Soetens, Schröter, & Sommer, 2002; Torres-Quesada, Milliken, Lupiáñez, & Funes, 2014). Most research on cognitive control has focused on individual brain areas, but cognitive control is a complex process involving large scale networks comprised of many brain regions that operate together (Kerns, 2006; Jiang & Egner, 2014; Töllner et al., 2017).

*Corresponding author: John Myers, Ph.D., Baylor College of Medicine, Department of Neurosurgery, Houston, TX 77030, john.myers@bcm.edu.

Conflict of interest: The authors declare that this research was conducted in the absence of any known conflicts of interest.

In this study, we tested the hypothesis that a large scale functional brain network could be identified using EEG during a cognitive control task, and that connectivity across this network would change dynamically in accordance with task demands.

The medial prefrontal cortex (mPFC) and anterior cingulate cortex (ACC) are important for cognitive control, as evidenced by neuroimaging and lesion studies (Ridderinkhof, Ullsperger, Crone, & Nieuwenhuis, 2004; Cohen, Ridderinkhof, Haupt, Elger, & Fell, 2008; di Pellegrino, Ciaramelli, & Làdavas, 2007). The ACC and mPFC are anatomically well-positioned to interact with sensory and motor regions and could dynamically influence many processes as cognitive control shifts (Brass & Haggard, 2008; Orr & Banich, 2014). Previous research suggests that the mPFC interacts with parietal regions during spatial conflict (Cohen & Ridderinkhof, 2013) and that within the PFC there may also be a rostral-caudal hierarchical organization that modulates cognitive control (Badre & Nee, 2018). Less is known about the time course of widespread cortical interactions and their connection to behavior.

Electrophysiological tools with high temporal resolution, such as scalp EEG and electrocorticography (ECoG), have been used to study neural oscillations during cognitive control (Cohen & Ridderinkhof, 2013; Smith, et al., 2019; Töllner et al., 2017). Spectral power within the mPFC and ACC is modulated during cognitive control, especially within the theta band (~3-8 Hz) (Cavanagh, Cohen, & Allen, 2009; Cavanagh & Frank, 2014; Cohen, 2014; Cohen & Ridderinkhof, 2013; Hanslmayr et al., 2008; Töllner, 2017). Changes in theta power during stimulus-response conflict correspond to different ‘brain states’ (Klimesch, 1999), where synchronous fluctuations in membrane potential within a given brain area might reflect attentional selectivity and expectancy (Engel, Fries, & Singer, 2001). Töllner and colleagues (2017) reported increased theta power in the mPFC and ACC during cognitive control and changes in ACC theta power during conflict adjustments. However, theta coherence across larger scale networks has not been thoroughly investigated, and the brain-behavior connections remain obscure.

Neuronal coherence is a mechanism for network-level connectivity, where brain areas oscillate in-phase to transfer information (Fries, 2005; 2015). Medial frontal theta coherence reflects cognitive control and varies with task demands (Cavanagh, Cohen, & Allen, 2009; Cohen, 2014; Womelsdorf et al., 2007). For instance, theta coherence between mPFC and lateral PFC increases during Flanker task error trials (Cavanagh et al., 2009). In laboratory settings, Stroop, Flanker, and Simon tasks (Eriksen & Eriksen, 1974; Simon & Rudell, 1967; Stroop, 1935) induce cognitive control by creating conflict between representations that influence response selection. The Simon task evokes cognitive control by introducing a spatial conflict between the stimulus location and response locations (typically left or right). On compatible trials, the stimulus is ipsilateral to the response hand; on incompatible trials, the stimulus is contralateral to the correct response hand. Spatial conflict on incompatible trials slows reaction time and reduces accuracy. However, behavioral performance improves on the trial after an incompatible trial (Clayson & Larson, 2011; Egner, 2007). One explanation for this post-conflict adaptation is that increased cognitive control on an incompatible trial modulates sensory and motor processing on the upcoming trial (Cole,

Yarkoni, Repovs, Anticevic, & Braver, 2012; Miller & Cohen, 2001). These theories have not been fully tested in large scale brain networks with high temporal resolution.

Here, we measured theta coherence during an auditory Simon task and performed source localization to examine functional connectivity of a comprehensive network of regions approximately localized to the ACC, mPFC, superior temporal gyrus (STG), supplementary motor area (SMA), posterior cingulate (PCC), and the inferior parietal lobe (IPL). Our primary hypothesis was that we would find functional connectivity between the ACC and mPFC, the magnitude of which would correlate with behavioral performance and which would increase with stimulus-response conflict. Additionally, we predicted that ACC and mPFC coherence, along with connectivity between the ACC or mPFC and other regions of interest, would vary based on current and previous amounts of conflict during the Simon task. Frontal theta has been implicated in cognitive control (Cavanagh & Frank, 2014), but less is known about the time course of control-related neural oscillations across the brain (Cohen, 2014). Therefore, we hypothesized that theta coherence (3-8 Hz) would increase between the ACC, mPFC, and other ROIs during stimulus-response conflict.

Material and Methods

Subjects

Subjects (N = 78) were university students that received extra credit for voluntary participation (mean age = 20.69 ± 3.05 years, 37 female, 75 right-handed). All subjects had normal hearing thresholds verified with audiometric testing (0.5–8.0 kHz). No participants reported a history of major psychiatric or neurological disorders. All subjects were given the Edinburgh Handedness Inventory (Oldfield, 1971).

Simon Task

We used an auditory task because spatial conflict is usually larger in the auditory modality, relative to the visual modality (Vu et al., 2003). Participants were introduced to two different white noise stimuli through insert earphones. One stimulus had an amplitude modulation (AM) rate of 25 Hz, which sounded similar to a card shuffle, and the other sounded more like a ‘buzz’ with a faster AM rate of 75 Hz (90% depth, 100–10,000 Hz, 200 ms duration, ~ 65 dB nHL, 5 ms rise/fall). A left and right button was assigned to each AM rate (counterbalanced across subjects). On each trial, the sounds were played in the left or right ear at 2.0 (n = 47) and 2.4 (n = 31) second intervals. Subjects were instructed to press the button with their corresponding hand to indicate the AM rate. On ‘compatible’ trials, the sound played on the same side as its button assignment (e.g. sound indicating left hand response button played in left ear). On ‘incompatible’ trials, the sound played to the ear opposite the correct response hand (e.g. left ear stimulus with sound indicating right hand response). Each trial was coded by both the previous and the current trial type, resulting in four permutations of compatible (C) vs. incompatible (IC) trials (i.e., C_C, C_IC, IC_C, and IC_IC). Participants received three (n = 47) or four (n = 31) blocks of 161 trials that each contained 50% compatible and 50% incompatible trials. Some participants also received three blocks each of 25% and 75% compatible trials not analyzed here (n = 47; Chinn et al., 2018). Trial 1 in each block was not analyzed because the analyses focused on sequence

effects. The order of the blocks containing each 'C' vs. 'IC' proportion was approximately counterbalanced across subjects. A practice block of 40 trials was given prior to testing.

Electrophysiological Data Acquisition

Electroencephalography (EEG) was recorded with a 64-channel Ag/AgCl electrode cap positioned according to the 10/20 system (Compumedics Neuroscan, Charlotte, NC). The cap contained a reference electrode between Cz and CPz. Additionally, four electrodes were placed near the lateral corners of each eye and above and below the left eye to detect electro-ocular activity. The EEG was recorded inside a sound attenuating, electrically shielded booth (IAC Acoustics, Bronx, New York) using Curry 7 Neuroimaging Suite Software (Compumedics Neuroscan, Charlotte, NC). The EEG data were digitized at 500 Hz with a DC-100 Hz band-pass filter.

EEG Data Processing

EEG data were recorded during the Simon task and processed offline with the EEGLAB (Delorme and Makeig, 2004) toolbox for Matlab (The Mathworks, Inc., Natick, MA). The data were high-pass filtered at 1 Hz, resampled to 250 Hz, epoched from −800 to 1200 ms (n = 47) or −800 ms to 1600 ms (n = 31) around stimulus onset, and average referenced. We visually inspected the data to exclude noisy channels and rejected epochs with excessive noise in the recording, ECG, or muscle activity and other non-stereotyped artifacts.

The underlying neural generators of scalp EEG are linearly mixed due to volume conduction (Brunner, Billinger, Seeber, Mullen, & Makeig, 2016). Therefore, estimating the brain-based origins of the signal requires linear decomposition and source localization methods (Cohen & Ridderinkhof, 2013; Jung et al., 2001; Wagner, Fuchs, & Kastner, 2004). Blind source separating using infomax independent component analysis (ICA) was performed on the EEG data to identify statistically independent components of the signal, thus mitigating the effects of volume conduction. Some independent components reflect physiologically distinct neural processes from specific brain regions, whereas others capture artifacts such as eye blinks (e.g., Bell and Sejnowski, 1995; Delorme and Makeig, 2004; Delorme et al., 2007; Jung et al., 2001). After ICA, the most probable location of each brain-based component was estimated from its best-fitting dipole (≤ 15% residual variance (RV)) within the standardized ICBM-MNI 152 head model using the 3-D EEG electrode coordinates and the boundary element method. The boundary element method serves as a numerical solution to the inverse problem of localizing neural sources while accounting for the conductive properties of brain, skull, and scalp (Oostenveld et al., 2011). To identify independent components indicative of neural activity, we selected components based on smooth scalp projections, physiologically plausible dipole locations, and spectral power curves that had a log-function shape in addition to peaks at theta, alpha, and beta frequency bands that classically reflect neural activity. RV constraints (≤ 15%) on IC dipole fitting ensured that all ICs reliably fit within standardized MNI brain space. Therefore, independent components localized to the eyes, facial or neck muscles, and ECG rhythms were not studied. We also visually inspected all components to ensure this was the case.

We combined two EEG datasets from the same auditory Simon task. One had a 2 second inter-trial interval (ITI) and the other had a 2.4 second ITI. Before combining the datasets, we tested whether the results of independent component analysis (ICA), k-means clustering, and spectral analysis would be replicated (Figure S1). To accomplish this, we first ran ICA, clustered each dataset individually (method described below), and compared the patterns of neuronal coherence between the two data sets. The results of the two cluster analyses were very similar, with the only exception being a main effect of ITI on coherence between the ACC and the PCC/precuneus, $F_{(1, 53)} = 11.061$, $p = 0.002$, $\eta_p^2 = 0.15$. Theta coherence was higher between the ACC and PCC/precuneus when the ITI was shorter, but conflict-related effects (i.e., compatible vs. incompatible) were the same across the two datasets. Therefore, we combined the datasets to address the underlying questions related to cognitive control. The sample size of 78 excludes the data of 13 subjects which could not be analyzed due to technical issues with the EEG recording, such as cap fitting and extensive motion artifacts. One subject's data was excluded due to a self-reported diagnosis of Asperger's Syndrome.

Regions of Interest (ROI) Analysis

Regions of interest (ROIs) were found using a k-means clustering algorithm based on the dimensionality derived from a principal component analysis (PCA). To maximize the probability that each dimension of the PCA was biased towards neural activity from a specific brain area, the estimated dipole location of each independent component (i.e., MNI coordinates) was weighted three times as heavily as the scalp map, power spectra, and ERSP. Outliers were removed from the final set if they were > 3 standard deviations from the mean features. The number of clusters k was set so that there would be an average of one IC computed per subject per cluster. The value of k was 8 clusters, meaning that on average each subject contributed 8 ICs. Clusters were selected only if they were consistently localized to the same brain regions across increasing values of k ($k = 7{:}14$) and contained ICs from more than 75% of the subjects. Seven clusters were selected based on these criteria. In cases where a single subject contributed more than one component to a cluster, we selected only the IC with the dipole location nearest the cluster centroid. This technique ensures that each subject is represented only once per ROI and benefits the anatomical interpretability of the results due to improved spatial centrality of each cluster. The final seven clusters contained neural sources from 83.7% of the subjects, ranging from 79.5% to 87.2%. Source data across subjects within each cluster were interpreted as local activity from the corresponding ROI (see Figure 1). The ROIs were the medial prefrontal cortex (mPFC), anterior cingulate cortex (ACC), left supplementary motor area (SMA), left superior temporal gyrus (STG), right sensorimotor cortex (SMC), right precuneus/posterior cingulate (PCC), and the right inferior parietal lobe (IPL).

Time-frequency Decomposition and Neuronal Coherence

Time-frequency decomposition was computed with Morlet wavelet convolution. Wavelet cycles were 3 Hz with 0.5 Hz increases for every 1 Hz increase in signal frequency. We measured theta oscillations (3-8 Hz) because, as noted above, evidence suggests that the mPFC and ACC are the underlying neural generators of EEG mid-frontal theta (Cohen, 2014; Töllner et al., 2017). Additionally, the phase of theta oscillations has been shown to influence information processing within brain regions by modulating activity at higher

frequencies, which are more correlated with neuronal spike timing (e.g., gamma oscillations) (e.g., Benchenane et al., 2010; Canolty et al., 2006). Neuronal coherence was measured between all ROIs and the mPFC versus ACC as an indicator of the phase synchrony related to cognitive control. Coherence is a power-based measure of phase synchrony given by $|xy|^2/|xx||yy|$, where the numerator corresponds to the average cross-spectrum and the denominator contains a normalization factor (Bendat, & Piersol, 2000; Srinivasan et al., 2007). For each variable (i.e., pair of brain regions), a single fixed time window of 200 ms duration was selected based on the point of maximum coherence across all subjects and behavioral conditions. Coherence data was averaged across the fixed time window.

Statistical Analysis

Neuronal coherence was averaged across the time windows of interest to quantify the data for each subject. A repeated-measures 2 (current trial: C vs. IC) x 2 (previous trial: C vs. IC) analysis of variance (ANOVA) was used to evaluate congruency sequence effects in behavioral response time and then in coherence between ROIs (C_C, C_IC, IC_C, IC_IC). A Bonferroni correction was used to correct for multiple comparisons across behavioral conditions for each ROI pair, and false discovery rate (FDR) correction was applied to control for multiple comparisons across ROIs. The ROI clusters in the mPFC (n = 65), ACC (n = 68), left SMA (n = 66), left STG (n = 62), right SMC (n = 63), right PCC (n = 67), and the right IPL (n = 66) contained an average of 83.7% of the subjects. Coherence analyses were only performed for data where subjects had ICs in both ROIs. To test the relationship between coherence measures and behavioral performance, we used Pearson correlations and ordinary least squares (OLS) regression. Statistical analyses were performed in SPSS. We were only interested in the neural mechanisms of successful cognitive control, so trials with incorrect behavioral responses were excluded from analysis.

Results

As hypothesized, our regions of interest (ROIs) derived from EEG data using ICA, source localization, and clustering of independent components across subjects included the mPFC and ACC. Additional ROIs were identified in the left SMA, right SMC, left STG, right precuneus/PCC, and right IPL, which also corresponded to our broader predictions of finding clusters in supplementary motor areas and the PCC (see Figure 1). Cognitive control adjustments are inferred below from congruency sequence effects, analyzed as the previous x current trial interaction.

Behavioral Effects

We first analyzed the behavioral data, which replicated previous congruency sequence effect studies by showing that the RT Simon effect was larger following compatible trials relative to incompatible trials ($F_{(1, 77)} = 193.9$, $p < 0.001$; See Figure 2). The sequence effect size was very large (Cohen's d = 1.41), and 73/78 subjects had larger Simon effects on trials after a compatible vs. incompatible trial. Having established robust behavioral effects that show adjustments to cognitive control across trials, we continued with analyses of cortical network-level activities associated with the sequence effects. These large behavioral effects observed in our cohort (see Chinn et al., 2018 and Figure 2) provided ample statistical power

to look at individual differences in reaction time relative to theta coherence and cognitive control demands in further analyses.

Neural Effects

Neuronal coherence between the mPFC and the ACC was higher when the current trial was incompatible, signifying the increased need for cognitive control (250-450 ms; $F_{(1, 56)} = 31.51$, $p = 0.002$, $\eta_p^2 = 0.36$). mPFC-ACC coherence peaked nearly 130 ms before the median RT across subjects (323 ms vs. 456 ms; $F_{(1, 112)} = 55.55$, $p < 0.001$, $\eta_p^2 = 0.32$). In accordance with slower RTs for incompatible trials, MFC-ACC coherence took longer to reach its peak when the current trial was incompatible (363 ms) vs. compatible (283 ms; $F_{(1, 56)} = 14.91$, $p < 0.001$, $\eta_p^2 = 0.21$). During auditory stimulus processing on incompatible current trials, the ACC increased coherence with the left STG (400-600 ms; $F_{(1, 57)} = 29.83$, $p = 0.002$, $\eta_p^2 = 0.34$). Additionally, the time courses of mPFC-ACC and ACC-STG coherence varied according to the current trial type. If the current trial was compatible, then mPFC-ACC coherence reached peak latency ~50 ms *before* ACC-STG coherence (283 ms vs. 330 ms). If the current trial was incompatible then mPFC-ACC coherence peaked ~20 ms *after* ACC-STG coherence (363 ms vs. 342 ms), as indicated by a significant coherence pair (MFC-ACC vs. ACC-STG) x trial type interaction ($F_{(1, 105)} = 4.77$, $p < 0.031$, $\eta_p^2 = 0.04$; see Figure 3). The interaction effect provides evidence that stimulus-response conflict extends the duration of control-related processing in mPFC-ACC beyond the time course of stimulus processing. The right precuneus/PCC was also more synchronized with the mPFC ($F_{(1, 55)} = 13.71$, $p = 0.002$, $\eta_p^2 = 0.20$). A main effect of 'previous trial' showed that mPFC-ACC coherence was increased when the previous trial was incompatible (250-450 ms; $F_{(1, 56)} = 14.05$, $p < 0.001$, $\eta_p^2 = 0.20$). Coherence between the ACC and left STG was also higher when the previous trial was compatible (350-550 ms; $F_{(1, 57)} = 10.12$, $p = 0.002$, $\eta_p^2 = 0.15$).

Adjustments in cognitive control between previous and current trials were best accounted for by coherence between the ACC and other brain areas. mPFC-ACC coherence was highest when the current trial was incompatible but the previous trial was compatible (250-450 ms; $F_{(1, 56)} = 22.27$, $p = 0.001$, $\eta_p^2 = 0.29$; see Figure 3). While adjusting cognitive control to account for stimulus-response conflict, the left STG ($F_{(1, 56)} = 10.07$, $p = 0.007$, $\eta_p^2 = 0.16$) and the left SMA ($F_{(1, 56)} = 14.43$, $p = 0.001$, $\eta_p^2 = 0.21$) both showed increased neuronal coherence with the ACC (see Figures 3 & 4). The interactions suggest that the ACC monitors stimulus-response conflict based on previous vs. current information and that the ACC conveys information to the mPFC in order to instantiate cognitive control on the current trial. Congruency sequence effects were best explained by coherence between the ACC, left STG, left SMA, and mPFC (Figure S2).

Brain-Behavior Correlations

mPFC-ACC coherence predicted individual differences in median RT. A negative correlation between mPFC-ACC coherence and median RT across subjects ($r = -0.282$, $p = 0.046$) suggests that higher coherence between these control-related brain regions can lead to faster responses at the individual level. For each trial type (C_C, C_IC, IC_C, IC_IC), linear regression was computed with mPFC-ACC coherence as the predictor and overall median

RT as the dependent variable (see Figure 5). The ability to sustain mPFC-ACC coherence on IC_C trials consistently predicted RT, $F_{(1, 56)} = 7.89$, $p = 0.028$, $r^2 = 0.13$, but the ability to increase coherence on C_IC trials was also a predictor of RT, $F_{(1, 55)} = 6.39$, $p = 0.028$, $r^2 = 0.10$. Intriguingly, mPFC-ACC coherence on C_C trials had no linear relationship with RT ($r^2 = 0.001$, $p = 1.00$), suggesting that neuronal coherence between the mPFC and ACC has a greater effect on RT when stimulus-response conflict is either present on the current or previous trial (see Figure 5). People who responded faster sustained higher mPFC-ACC coherence after experiencing stimulus-response conflict on previous trials that were incompatible, and they also showed greater increases in mPFC-ACC coherence when adjusting for current stimulus-response conflict (see Figure 5). We also found that ACC-left SMA coherence on IC_C trials predicted median RT ($F_{(1, 55)} = 7.31$, $p = 0.024$, $r^2 = 0.12$), showing a noticeably stronger negative correlation across subjects than mPFC-ACC coherence ($r = -0.384$, $p = 0.003$). Even in the absence of conflict on C_C trials, ACC-left SMA coherence was a trending predictor of overall reaction time ($r^2 = 0.061$, $p = 0.065$), implying that a functional connection between the ACC and left SMA is related to response selection in general and is less specific to conflict detection. The peak latency of ACC-left SMA coherence on C_IC trials negatively correlated with overall accuracy ($r = -0.318$, $p = 0.026$; see Figure 6). Subjects with more accurate responses showed shorter peak latency between the ACC and left SMA on C_IC trials.

Discussion

We examined functional connectivity in a widespread cortical network that subserves spatial cognitive control. Theta coherence (3-8 Hz) was measured between source localized EEG activity for precise temporal tracking of co-activation among brain regions. We found robust dipoles localized to mPFC and ACC in many subjects. These areas have been linked to cognitive control in previous studies (e.g., Kerns et al., 2004; Töllner et al., 2017). Strong theta coherence between the mPFC and ACC was present during stimulus-response conflict. Coherence involving the mPFC, ACC, right inferior parietal lobe (IPL), right sensorimotor cortex (SMC), and left superior temporal gyrus (STG) changed dynamically based on previous and current stimulus features, together forming a widespread network of brain regions to ensure accurate and timely response selection. Only the ACC showed significant changes in coherence when adjusting for both previous and current conflict. These results suggest that ACC monitors stimulus- and response-related information based on previous and current events, serving as an informational hub between the mPFC, sensory (STG) and motor planning (SMA) areas. Results suggest that together, these brain regions coordinate successful task performance.

Our primary hypothesis that functional connectivity between the ACC and mPFC would correlate with behavioral performance and increase with stimulus-response conflict was supported. ACC-mPFC coherence was greater, and peaked later, when adjusting to stimulus-response conflict after trials without conflict. This interaction suggests that ACC-mPFC coherence is sensitive to both previous and current information, especially when the need for cognitive control is greater. This result supports previous fMRI and lesion studies suggesting that the ACC and frontal cortex form a cognitive control network (Gläscher et al., 2012; Kerns, 2006). ACC-mPFC coherence also mapped onto behavioral performance. When

conflict occurred on either the previous or current trial, ACC-mPFC coherence showed a negative correlation with RT, which indicates that increased communication between these regions is directly connected to processing speed when conflict has recently occurred.

This study has provided new evidence that ACC and mPFC rapidly communicate prior to behavioral action, and they synchronize with lateral and posterior brain regions in response to previous and current compatibility information. Most subjects in this study had dipoles localized to the left STG, and we found a significantly larger effect of current trial conflict when the previous trial was compatible relative to when it was incompatible (Previous x Current trial interaction) in ACC-left STG coherence. This result suggests coherence between the ACC and STG can encodes information both previous and current auditory stimuli. Notably, less than 40% of participants had sources localized to the right STG, which suggests a specialized functional laterality for the left STG. This finding aligns with previous research showing that the left STG responds differently to task-related deviant sounds than the right STG, for both speech (Hickock & Poeppel, 2007) and non-speech sounds (Levänen et al., 1996).

As noted above, one limitation of EEG is that it has lower spatial resolution relative to neuroimaging methods such as MRI and invasive techniques such as electrocorticography (ECoG). Findings from ICA and source localization permit inferences about the brain regions involved in these cognitive control network, with a caveat that localization is based on lower resolution EEG signals. However, since the mPFC and ACC dipole locations agreed with neuroimaging findings in similar cognitive control tasks (e.g., Jiang and Egner, 2014; Kerns, 2006), it is reasonable that these areas were correctly localized. The location of these prefrontal dipoles also aligns with models that implicate a rostral-caudal hierarchical organization that supports cognitive control (Badre & Nee 2018), which associate caudal ACC with stimulus-response conflict (Jiang and Egner, 2014). Another important limitation of this study is its reliance on coherence analyses. Although there were large effects of cognitive control demands on synchrony between brain regions, our analyses did not establish causal influences for relations between ACC and mPFC and neural activity in the other ROIs. The directionality of information flow must be evaluated with other methods, such as Granger causality. Future studies using scalp EEG, intracranial ECoG, or stereotactic EEG could expand knowledge on the information flow involved in spatial cognitive control.

Some brain regions showed increased theta coherence only in response to features of the previous or current trial, without any interaction between the two conditions. Coherence between the ACC and right IPL was higher overall on a given trial when the previous trial was compatible. The right IPL is important for spatial cognition (Husain & Nachev, 2007), so ACC-IPL coherence could be involved in representing the spatial location of the previous stimulus.

In addition to sensory areas, our results suggest that sensorimotor planning is also driven by neuronal coherence. Specifically, theta coherence between the mPFC and right SMC tended to decrease when the previous trial was incompatible. Reaction times were also slower when the previous trial was incompatible. Perhaps this reduced mPFC-motor coherence is associated with temporary inhibition of motor responses in order to proactively avoid errors.

With respect to current trial response selection, mPFC-right SMC coherence was higher when the current trial was incompatible, which may indicate increased communication between regions involved in response selection and motor control. Task demands also affected the peak latency of coherence. ACC-left STG coherence peaked later than ACC-mPFC coherence, primarily during C_IC trials (Figure 3a). This result suggests that an increase in the need for cognitive control may extend the duration of control-related processing beyond the average time course of more basic stimulus processing in the STG.

We expanded on previous results linking the ACC and mPFC to cognitive control (e.g. Botvinick, Cohen, & Carter, 2004; Botvinick, Braver, Barch, Carter, & Cohen, 2001) by relating neuronal coherence to individual differences in behavioral performance, at the subject level. Subjects with faster overall responses showed more ACC-mPFC theta coherence. The negative correlation between ACC-mPFC coherence and RT highlights the importance of stronger coupling between the mPFC and ACC for efficient conflict processing. A previous scalp EEG study showed that at the single trial level, higher midline theta power was associated with higher levels of conflict and longer reaction times in a Flanker task (Cohen & Cavanagh, 2011). Our results also expand on those discoveries.

Widespread theta coherence during accurate task performance has also been observed in a recent ECoG study (Solomon et al., 2017). In accordance with those findings, we discovered that the peak latency of ACC-left SMA coherence, specifically during C_IC trials, predicted individual differences in accuracy. Subjects with more accurate responses had earlier peaks in ACC-left SMA coherence, suggesting that correct response selection may be related to the efficiency of communication between the ACC and SMA. The effects linking neuronal coherence to individual differences in RT and accuracy may have implications for understanding the relationship between cognitive control and human intelligence. In similar choice reaction time tasks, fluid intelligence has been associated with faster RTs (Schulz-Zhecheva et al., 2016).

The mPFC is known to generate theta oscillations (see Cohen, 2014). Animal studies show that layer V cells in this region have denser local connectivity compared to sensory processing regions such as visual cortex, and their dendrites terminate in more superficial input layers (Wang et al., 2006). In response to input currents, the mPFC also oscillates at a theta rhythm (Dembrow, Chitwood, & Johnston, 2010; Silva et al., 1991). In the ACC, theta power predicts adjustments to task rules, and theta coherence between the prefrontal cortex and the hippocampus can modulate prefrontal spike timing during memory formation (Womelsdorf et al., 2010). Taken together, the research suggests that long range theta coherence is dynamically modulated to represent previous and current task-related information. The results of this study provide strong evidence that the time course of neuronal coherence is a key mechanism for understanding how cognitive control is instantiated across a widespread network of brain regions.

Supplementary Material

Refer to Web version on PubMed Central for supplementary material.

Acknowledgments:

This study was supported in part by NSF CAREER award BCS-0844961, NIH R01DC014736, and Tulane Flowerree Summer Research Fellowships. Carolyn Pauker collected a portion of the data in this study.

Data and code availability:

The data analyzed during the current study are available from the corresponding author on reasonable request. Code used in this study can be found at https://github.com/john-myers-github/Spatial_CogControl

References

Badre D, & Nee DE (2018). Frontal Cortex and the Hierarchical Control of Behavior. Trends in Cognitive Sciences, 22 (2), 170–188. 10.1016/j.tics.2017.11.005 [PubMed: 29229206]

Bell a J., & Sejnowski TJ (1995). An information-maximization approach to blind separation and blind deconvolution. Neural Computation, 7(6), 1129–1159. 10.1162/neco.1995.7.6.1129 [PubMed: 7584893]

Benchenane K, Peyrache A, Khamassi M, Tierney PL, Gioanni Y, Battaglia FP, & Wiener SI (2010). Coherent theta oscillations and reorganization of spike timing in the hippocampal-prefrontal network upon learning. Neuron, 66(6), 921–936. 10.1016/j.neuron.2010.05.013 [PubMed: 20620877]

Bendat JS, & Piersol AG (2000). Random data: analysis and measurement procedures. John Wiley & Sons: Hoboken, New Jersey.

Botvinick M, Cohen J, & Carter C (2004). Conflict monitoring and anterior cingulate cortex: an update. Trends in Cognitive Sciences. 10.1016/j.tics.2004.10.003

Botvinick MM, Braver TS, Barch DM, Carter CS, & Cohen JD (2001). Conflict monitoring and cognitive control. Psychological Review, 108(3), 624–652. 10.1037/0033-295X.108.3.624 [PubMed: 11488380]

Brass M, & Haggard P (2008). The what, when, whether model of intentional action. The Neuroscientist, 14(4), 319–325. 10.1177/1073858408317417 [PubMed: 18660462]

Brunner C, Billinger M, Seeber M, Mullen TR, & Makeig S (2016). Volume Conduction Influences Scalp-Based Connectivity Estimates. Frontiers in Computational Neuroscience, 10, 121. 10.3389/fncom.2016.00121 [PubMed: 27920674]

Canolty RT, Edwards E, Dalal SS, Soltani M, Nagarajan SS, Kirsch HE, Berger MS, Barbaro NM, & Knight RT (2006). High gamma power is phase-locked to theta oscillations in human neocortex. Science, 313(5793), 1626–1628. 10.1126/science.1128115 [PubMed: 16973878]

Cavanagh JF, Cohen MX, & Allen JJB (2009). Prelude to and Resolution of an Error: EEG Phase Synchrony Reveals Cognitive Control Dynamics during Action Monitoring. Journal of Neuroscience, 29(1), 98–105. 10.1523/JNEUROSCI.4137-08.2009 [PubMed: 19129388]

Cavanagh JF, & Frank MJ (2014). Frontal theta as a mechanism for cognitive control. Trends in Cognitive Sciences, 1–8. 10.1016/j.tics.2014.04.012

Chinn LK, Pauker CS, & Golob EJ (2018). Cognitive control and midline theta adjust across multiple timescales. Neuropsychologia, 111. 10.1016/j.neuropsychologia.2018.01.031

Clayson PE, & Larson MJ (2011). Conflict adaptation and sequential trial effects: Support for the conflict monitoring theory. Neuropsychologia, 49(7), 1953–1961. 10.1016/j.neuropsychologia.2011.03.023 [PubMed: 21435347]

Cohen MX (2014). A neural microcircuit for cognitive conflict detection and signaling. Trends in neurosciences, 37(9), 480–490. 10.1016/j.tins.2014.06.004 [PubMed: 25034536]

Cohen MX, & Cavanagh JF (2011). Single-trial regression elucidates the role of prefrontal theta oscillations in response conflict. Frontiers in Psychology 2, 30. 10.3389/fpsyg.2011.00030 [PubMed: 21713190]

Cohen MX, & Ridderinkhof KR (2013). EEG source reconstruction reveals frontal-parietal dynamics of spatial conflict processing. PloS One, 8(2), e57293. 10.1371/journal.pone.0057293 [PubMed: 23451201]

Cohen MX, Ridderinkhof KR, Haupt S, Elger CE, & Fell J (2008). Medial frontal cortex and response conflict: evidence from human intracranial EEG and medial frontal cortex lesion. Brain research, 1238, 127–142. 10.1016/j.brainres.2008.07.114 [PubMed: 18760262]

Cole MW, Yarkoni T, Repovs G, Anticevic A, & Braver TS (2012). Global connectivity of prefrontal cortex predicts cognitive control and intelligence. The Journal of Neuroscience : The Official Journal of the Society for Neuroscience, 32(26), 8988–99. 10.1523/JNEUROSCI.0536-12.2012 [PubMed: 22745498]

Delorme A, & Makeig S (2004). EEGLAB: an open source toolbox for analysis of single-trial EEG dynamics including independent component analysis. J Neurosci Methods, 134(1), 9–21. 10.1016/j.jneumeth.2003.10.009 [PubMed: 15102499]

Delorme A, Sejnowski T, & Makeig S (2007). Enhanced detection of artifacts in EEG data using higher-order statistics and independent component analysis. NeuroImage 34(4), 1443–1449. 10.1016/j.neuroimage.2006.11.004 [PubMed: 17188898]

Dembrow NC, Chitwood RA, & Johnston D (2010). Projection-specific neuromodulation of medial prefrontal cortex neurons. Journal of Neuroscience, 30(50), 16922–16937. 10.1523/JNEUROSCI.3644-10.2010 [PubMed: 21159963]

di Pellegrino G, Ciaramelli E, & Làdavas E (2007). The Regulation of Cognitive Control following Rostral Anterior Cingulate Cortex Lesion in Humans. Journal of Cognitive Neuroscience, 19(2), 275–286. 10.1162/jocn.2007.19.2.275 [PubMed: 17280516]

Egner T (2007). Congruency sequence effects and cognitive control. Cognitive, Affective, & Behavioral Neuroscience, 7(4), 380–390. 10.3758/CABN.7.4.380

Egner T, & Hirsch J (2005). Cognitive control mechanisms resolve conflict through cortical amplification of task-relevant information. Nature neuroscience, 8(12), 1784. 10.1038/nn1594 [PubMed: 16286928]

Engel AK, Fries P, & Singer W (2001). Dynamic predictions: oscillations and synchrony in top–down processing. Nature Reviews Neuroscience, 2(10), 704. 10.1038/35094565 [PubMed: 11584308]

Eriksen BA, & Eriksen CW (1974). Effects of noise letters upon the identification of a target letter in a nonsearch task. Perception & Psychophysics, 16(1), 143–149. 10.3758/BF03203267

Fries P (2005). A mechanism for cognitive dynamics: neuronal communication through neuronal coherence. Trends in Cognitive Sciences, 9(10), 474–480. 10.1016/j.tics.2005.08.011 [PubMed: 16150631]

Fries P (2015). Rhythms for cognition: communication through coherence. Neuron, 88(1), 220–235. 10.1016/j.neuron.2015.09.034 [PubMed: 26447583]

Gläscher J, Adolphs R, Damasio H, Bechara A, Rudrauf D, Calamia M, Paul LK, & Tranel D (2012). Lesion mapping of cognitive control and value-based decision making in the prefrontal cortex. Proceedings of the National Academy of Sciences of the United States of America, 109(36), 14681–14686. 10.1073/pnas.1206608109 [PubMed: 22908286]

Golob EJ, & Mock JR (2019). Auditory spatial attention capture, disengagement, and response selection in normal aging. Attention, Perception, & Psychophysics, 81(1), 270–280. 10.3758/s13414-018-1611-y

Hanslmayr S, Pastötter B, Bäuml K-H, Gruber S, Wimber M, & Klimesch W (2008). The electrophysiological dynamics of interference during the Stroop task. Journal of Cognitive Neuroscience, 20(2), 215–225. 10.1162/jocn.2008.20020 [PubMed: 18275330]

Hickok G, & Poeppel D (2007). The cortical organization of speech processing. Nature Reviews Neuroscience, 8(May), 393–402. 10.1038/nrn2113 [PubMed: 17431404]

Hommel B (2011). The Simon effect as tool and heuristic. Acta Psychologica, 136(2), 189–202. [PubMed: 20507830]

Husain M, & Nachev P (2007). Space and the parietal cortex. Trends in cognitive sciences, 11(1), 30–36. 10.1016/j.tics.2006.10.011 [PubMed: 17134935]

Jiang J, & Egner T (2014). Using Neural Pattern Classifiers to Quantify the Modularity of Conflict–Control Mechanisms in the Human Brain. Cerebral Cortex, 24(7), 1793–1805. 10.1093/cercor/bht029 [PubMed: 23402762]

Jung T-P, Makeig S, Mckeown MJ, Bell AJ, Lee T-W, & Sejnowski TJ (2001). Imaging Brain Dynamics Using Independent Component Analysis. IEEE Proceedings, 88(7), 1107–22. 10.1109/5.939827

Kerns JG (2006). Anterior cingulate and prefrontal cortex activity in an FMRI study of trial-to-trial adjustments on the Simon task. NeuroImage, 33(1), 399–405. 10.1016/j.neuroimage.2006.06.012 [PubMed: 16876434]

Kerns JG, Cohen JD, MacDonald AW, Cho RY, Stenger VA, & Carter CS (2004). Anterior cingulate conflict monitoring and adjustments in control. Science, 303(5660), 1023–6. 10.1126/science.1089910 [PubMed: 14963333]

Klimesch W (1999). EEG alpha and theta oscillations reflect cognitive and memory performance: a review and analysis. Brain Res Brain Res Rev, 29(2–3), 169–195. 10.1016/S0165-0173(98)00056-3 [PubMed: 10209231]

Levänen S, Ahonen A, Hari R, McEvoy L, & Sams M (1996). Deviant auditory stimuli activate human left and right auditory cortex differently. Cerebral Cortex, 6(2), 288–296. 288-296. 10.1093/cercor/6.2.288 [PubMed: 8670657]

Miller EK, & Cohen JD (2001). An integrative theory of prefrontal cortex function. Annu Rev Neurosci, 24, 167–202. 10.1146/annurev.neuro.24.1.167 [PubMed: 11283309]

Oldfield RC (1971). The assessment and analysis of handedness: the Edinburgh inventory. Neuropsychologia 9(1), 97–113. 10.1016/0028-3932(71)90067-4 [PubMed: 5146491]

Oostenveld R, Fries P, Maris E, & Schoffelen J-M (2011). FieldTrip: Open source software for advanced analysis of MEG, EEG, and invasive electrophysiological data. Computational Intelligence and Neuroscience 2011, 156869. 10.1155/2011/156869 [PubMed: 21253357]

Orr JM, & Banich MT (2014). The neural mechanisms underlying internally and externally guided task selection. NeuroImage, 84, 191–205. 10.1016/J.NEUROIMAGE.2013.08.047 [PubMed: 23994316]

Ridderinkhof KR, Ullsperger M, Crone EA, & Nieuwenhuis S (2004). The Role of the Medial Frontal Cortex in Cognitive Control. Science, 306(5695), 443–447. 10.1126/science.1100301 [PubMed: 15486290]

Risko EF, Blais C, Stolz JA, & Besner D (2008). Nonstrategic contributions to putatively strategic effects in selective attention tasks. Journal of Experimental Psychology. Human Perception and Performance, 34(4), 1044–52. 10.1037/0096-1523.34.4.1044 [PubMed: 18665744]

Schulz-Zhecheva Y, Voelkle M, Beauducel A, Biscaldi M, & Klein C (2016). Predicting fluid intelligence by components of reaction time distributions from simple choice reaction time tasks. Journal of Intelligence, 4(3), 8. 10.3390/jintelligence4030008

Silva LR, Amitai Y, & Connors BW (1991). Intrinsic oscillations of neocortex generated by layer 5 pyramidal neurons. Science, 251(4992), 432–435. 10.1126/science.1824881 [PubMed: 1824881]

Simon JR, & Rudell AP (1967). Auditory S-R compatibility: The effect of an irrelevant cue on information processing. Journal of Applied Psychology, 51(3), 300–304. 10.1037/h0020586

Smith EH, Guillermo H, Yates MJ, Mikell CB, Banks GP, Pathak YJ, Schevon CA, McKhann GM II, Hayden BY, Botvinick MM, Sheth SA (2019). Widespread temporal coding of cognitive control in the human prefrontal cortex. Nature Neuroscience, 22, 1883–1891. 10.1038/s41593-019-0494-0 [PubMed: 31570859]

Solomon EA, Kragel JE, Sperling MR, Sharan A, Worrell G, Kucewicz M, Inman CS, Lega B, Davis KA, Stein JM, Jobst BC, Zaghloul KA, Sheth SA, Rizzuto DS, & Kahana MJ (2017). Widespread theta synchrony and high-frequency desynchronization underlies enhanced cognition. Nature communications, 8(1), 1704. 10.1038/s41467-017-01763-2

Srinivasan R, Winter WR, Ding J, & Nunez PL (2007). EEG and MEG coherence: measures of functional connectivity at distinct spatial scales of neocortical dynamics. Journal of Neuroscience Methods, 166(1), 41–52. 10.1016/j.jneumeth.2007.06.026 [PubMed: 17698205]

Stroop JR (1935). Studies of interference in serial verbal reactions. Journal of Experimental Psychology, 18(6), 643–662. 10.1037/h0054651

Stürmer B, Leuthold H, Soetens E, Schröter H, & Sommer W (2002). Control over location-based response activation in the Simon task: behavioral and electrophysiological evidence. Journal of Experimental Psychology. Human Perception and Performance, 28(6), 1345–63. 10.1037/0096-1523.28.6.1345 [PubMed: 12542132]

Töllner T, Wang Y, Makeig S, Müller HJ, Jung T-P, & Gramann K (2017). Two Independent Frontal Midline Theta Oscillations During Conflict Detection and Adaptation in a Simon-type Manual Reaching Task. J. Neurosci, 10, 1752–16. 10.1523/JNEUROSCI.1752-16.2017

Torres-Quesada M, Milliken B, Lupiáñez J, & Funes MJ (2014). Proportion Congruent effects in the absence of Sequential Congruent effects. Psicológica, 35, 101–115. 10.1016/j.actpsy.2014.03.006

Vissers ME, Ridderinkhof KR, Cohen MX, & Slagter HA (2018). Oscillatory mechanisms of response conflict elicited by color and motion direction: An individual differences approach. Journal of cognitive neuroscience, 30(4), 468–481. 10.1162/jocn_a_01222 [PubMed: 29244639]

Wagner M, Fuchs M, & Kastner J (2004). Evaluation of sLORETA in the presence of noise and multiple sources. Brain Topogr, 16(4), 277–280. 10.1023/B:BRAT.0000032865.58382.62 [PubMed: 15379227]

Wang Y, Markram H, Goodman PH, Berger TK, Ma J, & Goldman-Rakic PS (2006). Heterogeneity in the pyramidal network of the medial prefrontal cortex. Nature Neuroscience 9(4), 534–542. 10.1038/nn1670 [PubMed: 16547512]

Womelsdorf T, Schoffelen JM, Oostenveld R, Singer W, Desimone R, Engel AK, & Fries P (2007). Modulation of neuronal interactions through neuronal synchronization. Science, 316(5831), 1609–1612. 10.1126/science.1139597 [PubMed: 17569862]

Womelsdorf T, Vinck M, Leung LS, & Everling S (2010). Selective Theta-Synchronization of Choice-Relevant Information Subserves Goal-Directed Behavior. Frontiers in Human Neuroscience, 4, 210. 10.3389/fnhum.2010.00210 [PubMed: 21119780]

Highlights

- Cognitive control requires dynamic coordination across a widespread network of brain regions
- Phase synchrony, or coherence, between the medial prefrontal cortex (mPFC) and anterior cingulate (ACC) increases with task difficulty
- Coherence between the mPFC and ACC can predict individual differences in reaction time during a spatial cognitive control task
- Individual differences in accuracy were predicted by rapid activation of ACC-motor coherence, which highlights the relationship between cognitive processing speed and task performance

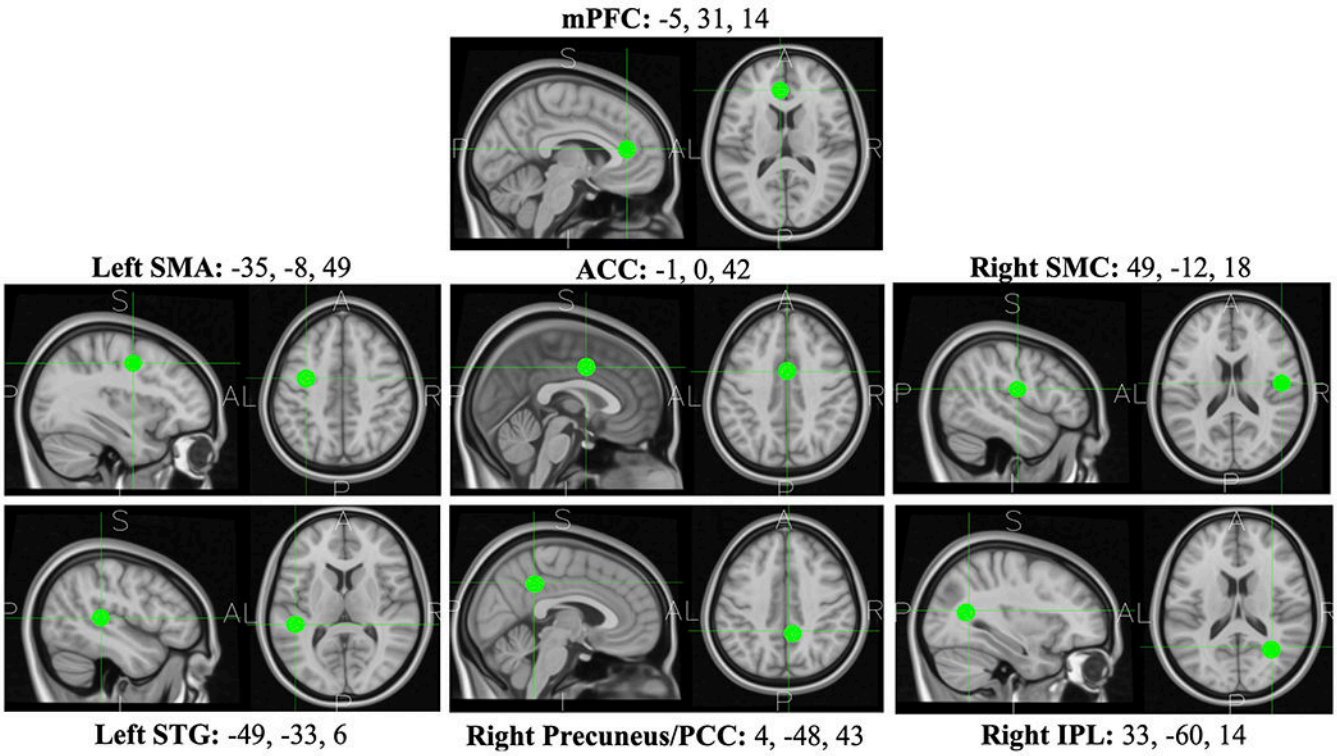

Figure 1. Regions of interest.

ROIs were derived via cluster analysis using the average best fitting dipole location of the neural source activity across subjects. The boundary element method was used to map the dipole location onto coordinates within the MNI space. MNI coordinates (x,y,z) are located above each T1-weighted image of the ROI.

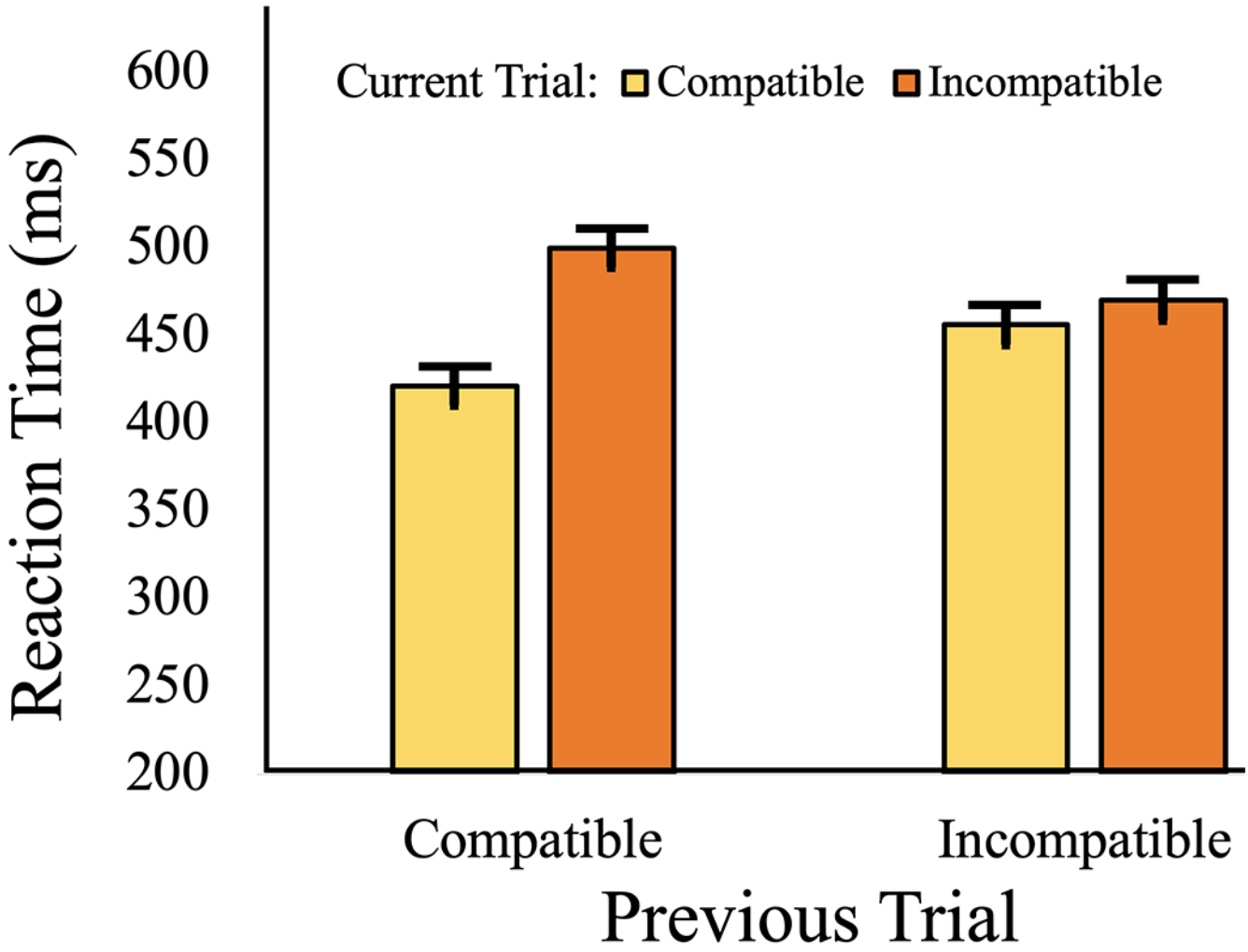

Figure 2. Congruency sequence effects on reaction time in milliseconds, shown by the current x previous trial type interaction (compatible, incompatible).

The left two bars illustrate a larger difference between the two current trial types when the previous trial was compatible, relative to the difference the previous trial was incompatible (right two bars; current x previous trial type interaction $p < .001$).

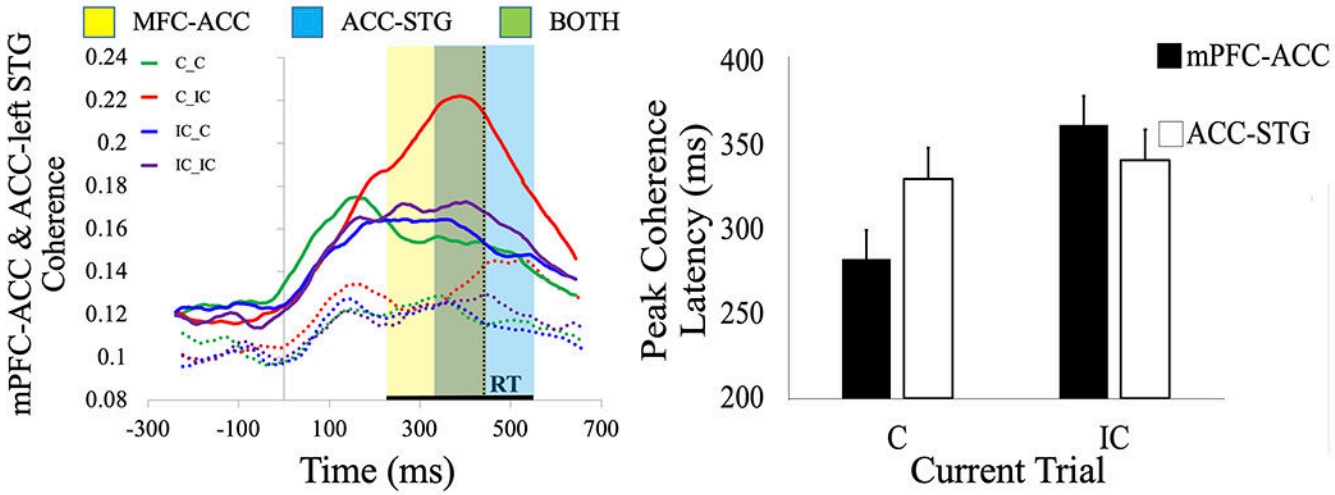

Figure 3. mPFC-ACC vs. ACC-STG coherence.

mPFC-ACC coherence (solid line) increased incrementally with level of conflict on the Simon task, being least on C_C trials and greatest on C_IC trials ($\eta_p^2 = 0.36$, $p < 0.001$). Similarly, ACC-STG coherence (dotted line) was highest on C_IC trials but in a later time window ($\eta_p^2 = 0.34$, $p < 0.001$) (A). The differences between time courses of coherence between the mPFC-ACC (yellow shade) vs. ACC-STG (blue shade) suggest that stimulus-response conflict is processed via synchronous theta oscillations between the mPFC and ACC, which extends the duration of cognitive processing for accurate response selection based on the auditory stimulus. Black horizontal line shows the median reaction time (RT) across participants. If the current trial was compatible, then mPFC-ACC coherence reached peak latency before ACC-STG coherence (330 ms vs. 283 ms) (B). If the current trial was incompatible, mPFC-ACC coherence peaked after ACC-STG coherence (342 ms vs. 363 ms) (interaction $\eta_p^2 = 0.04$, $p < 0.031$), which suggests that stimulus-response conflict extends the duration of control-related processing in mPFC-ACC beyond the time course of stimulus processing.

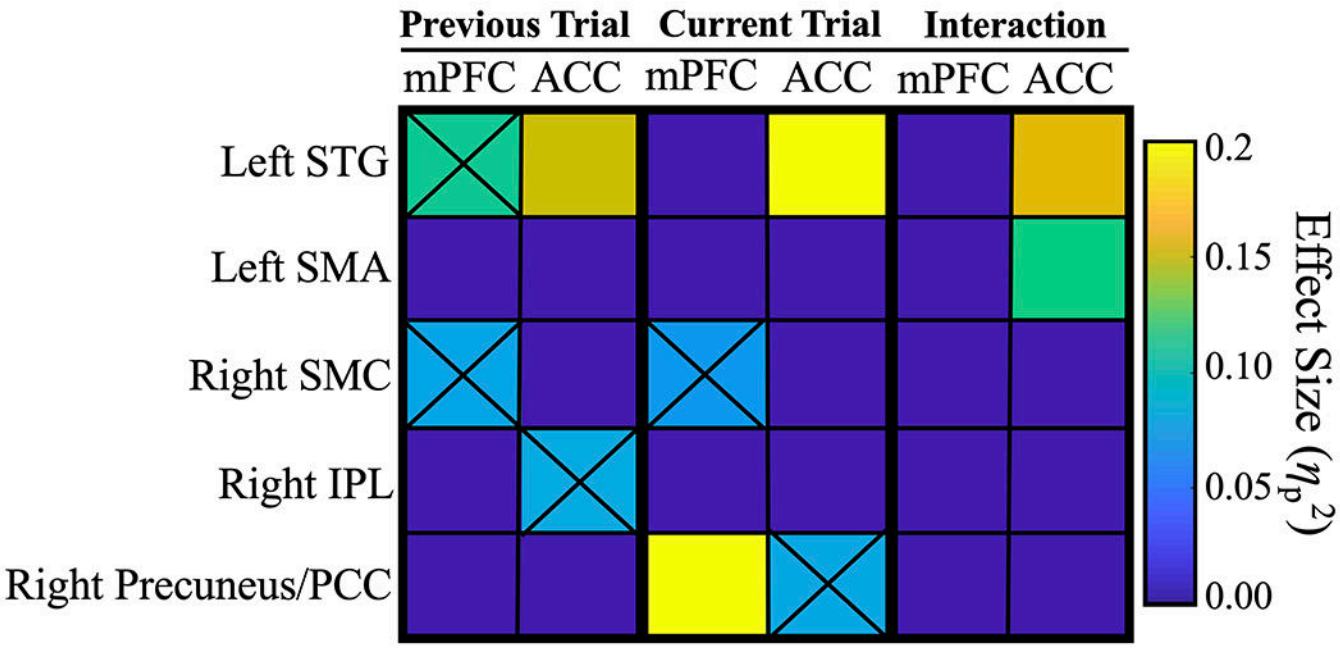

Figure 4. Congruency sequence effects (current x previous trial) within mPFC-ACC network.

Heatmap presents the effects of trial type on coherence between the mPFC-ACC and all ROIs (η_p^2). This visualization allows for separate evaluation of mPFC and ACC 'subnetworks' and sheds light on their functional relationship with temporal, parietal, and motor regions. Sensory information about previous and current auditory stimuli was important for cognitive control in this task. The ACC was tightly coupled to the left STG across all trials, which may indicate cognitive control-related stimulus processing. Similarly, synchrony with motor regions seemed necessary for accurate performance. Coherence adjustments (interaction effects) were found between the ACC and left SMA, which may represent action planning in order to optimize task performance. Black 'Xs' indicate the weaker coherence effects that were statistically significant prior to FDR correction.

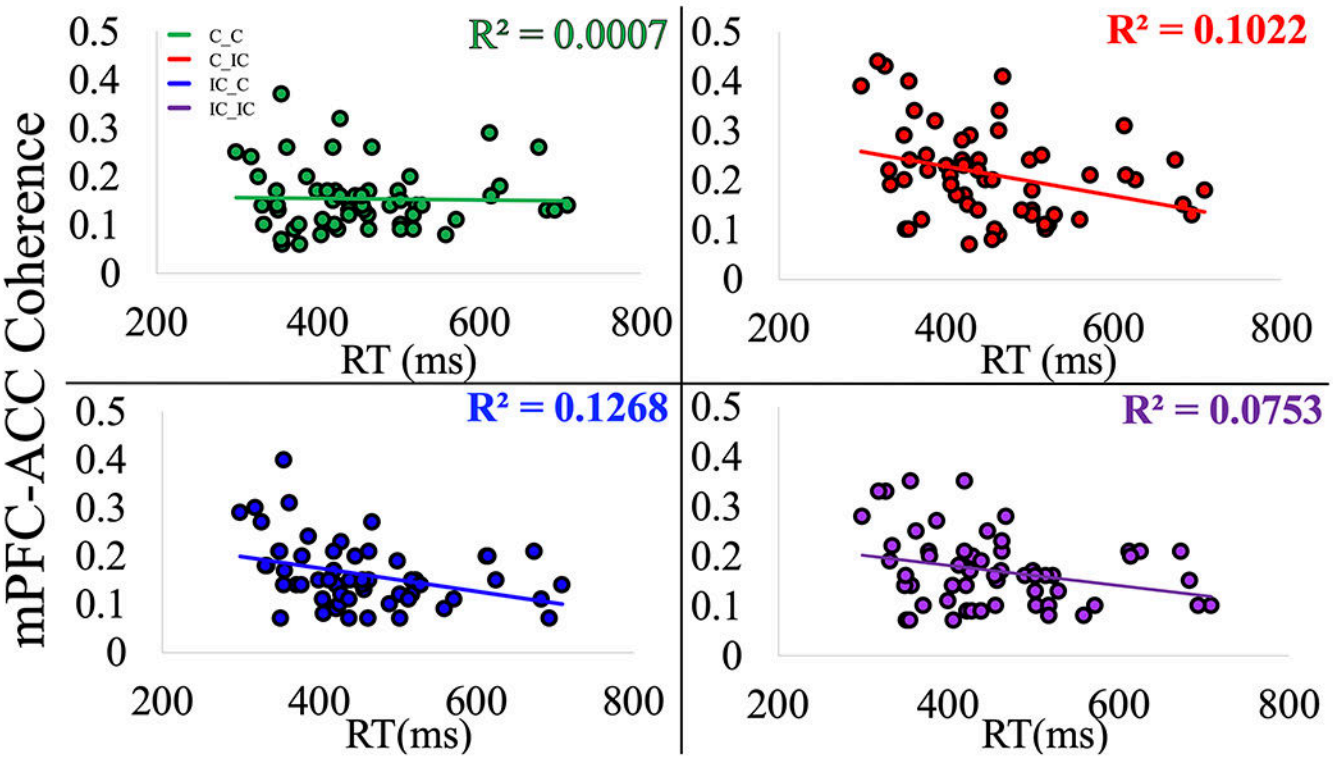

Figure 5. Effects of mPFC-ACC Coherence on Reaction Time.

When adjusting for conflict on a previous or current trial (C_IC, IC_C), mPFC-ACC coherence significantly predicted RT across subjects. People who responded faster sustained higher mPFC-ACC coherence after experiencing stimulus-response conflict on previous trials that were incompatible, and they also showed greater increases in mPFC-ACC coherence when adjusting for current stimulus-response conflict after previous trials with no conflict. The ability to sustain mPFC-ACC coherence on IC_C trials consistently predicted median RT ($p = 0.046$), but the ability to increase coherence on C_IC trials was also a predictor of RT, ($p = 0.028$). mPFC-ACC coherence on C_C trials showed no linear relationship with RT ($p = 1.00$). Theta coherence between the mPFC and ACC has a greater effect on RT when stimulus-response conflict is either present on the current or previous trial.

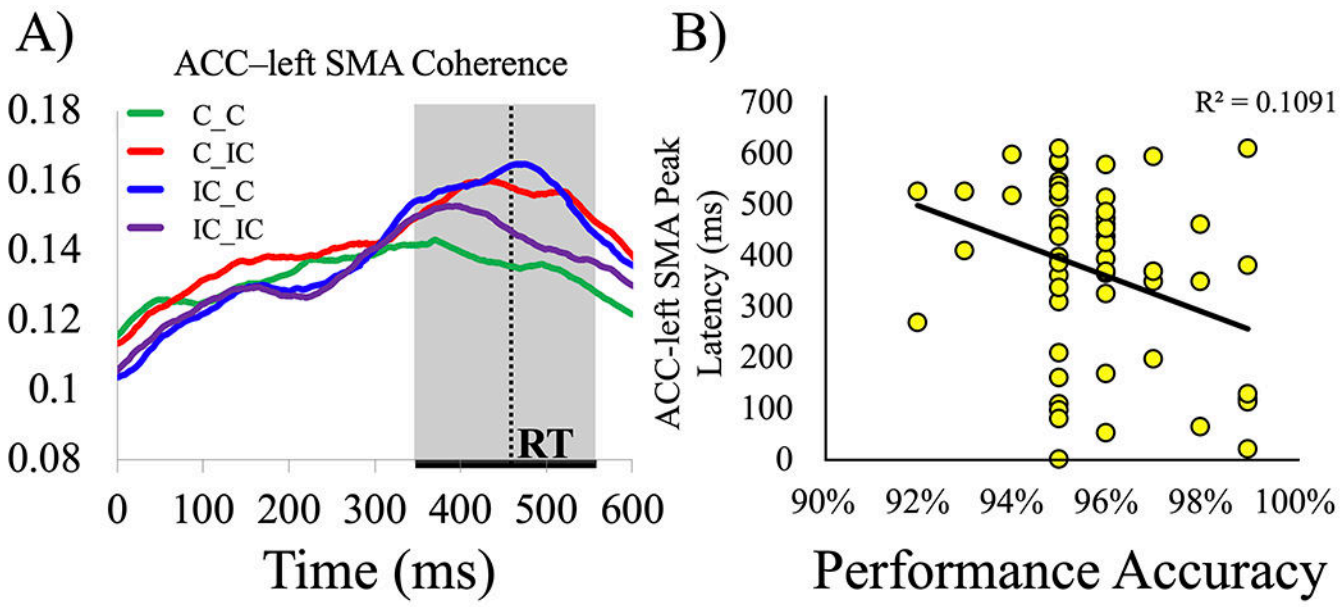

Figure 6. Effects of ACC-left SMA coherence.

ACC-left SMA coherence showed congruency sequence effects. (A). When the previous and current stimuli were the same trial type (compatible or incompatible), coherence was lower relative to when one trial was compatible and the other incompatible ($\eta_p^2 = 0.21$, $p = 0.001$). ACC-left SMA coherence on C_IC trials predicted individual differences in accuracy on the Simon task (B). Later peaks of cingulate-motor coherence were associated with less accurate responses across all trials ($r = -0.318$, $p = 0.026$). The ACC might convey task-related information to the SMA in preparation for more accurate responses in some subjects.